TIME-SERIES, STATISTICS AND SCALING OF PRESSURE, TEMPERATURE AND DENSITY FLUCTUATIONS IN COMPRESSIBLE WALL-TURBULENCE

G.A. Gerolymos [1] ***and D. Sénéchal*** [1]

[1] ***Université Pierre-et-Marie-Curie, 75005 Paris, France***

georges.gerolymos@upmc.fr

Abstract

The purpose of the present paper is to study the statistics and scalings of the fluctuations of thermodynamic quantities (pressure, density, temperature and entropy) in compressible wall-turbulence. Data were extracted from several DNS simulations of compressible turbulent channel flow ($Re_{\tau_w} \in [100, 500]$ and $\bar{M}_{\rm CL} \in [0.3, 2.5]$). We study 1-point and 2-point statistics, 1-point transport equations budgets, 2-time correlations and frequency-spectra. The appropriate scalings are discussed. Results with different resolutions and/or computational box sizes are compared and analyzed to draw guidelines on resolution requirements for the DNS of compressible wall-turbulence.

1 Introduction

Density-fluctuations are a direct measure of compressibility effects on turbulence (Taulbee and VanOsdol, 1991), and diffrentiate weakly compressible turbulent flows (Rubinstein and Erlebacher, 1997), where their relative importance is small, from flows with strong compressibility effects (Wu and Martín, 2007). An up-to-date review of DNS work on compressible turbulent flows was given by Friedrich (2007).

To understand the dynamics of density fluctuations in compressible wall-turbulence, it is necessary to study the dynamics of the fluctuations of different thermodynamics variables and their interaction. For general thermodynamic relations $p = p(\rho, T)$ and $c_p = c_p(\rho, T)$, the following relations hold between thermodynamic variables (Gerolymos et al., 2008)

$$dp = a^2 d\rho + \lambda_{\rm G} \rho T ds \tag{1a}$$

$$\rho c_p dT = \rho T ds + \beta_p T dp \tag{1b}$$

$$\rho c_p dT = (1 + \lambda_{\rm G} \beta_p T) \rho T ds + \beta_p T a^2 d\rho \tag{1c}$$

where a is the speed-of-sound, c_p is the heat capacity at constant pressure, β_p is the coefficient of thermal expansion (at constant pressure), and $\lambda_{\rm G}$ is the Grüneisen (Arp et al., 1984) parameter (expressible as a functions of the other 3 thermodynamic parameters)

$$a^2 = \left(\frac{\partial p}{\partial \rho}\right)_s \quad ; \quad c_p = \left(\frac{\partial h}{\partial T}\right)_p \tag{2a}$$

$$\beta_p = -\frac{1}{\rho}\left(\frac{\partial \rho}{\partial T}\right)_p \tag{2b}$$

$$\lambda_{\rm G} = \frac{\rho}{T}\left(\frac{\partial T}{\partial \rho}\right)_s = \frac{\beta_p a^2}{c_p} \tag{2c}$$

The well-known continuity and entropy production equations

$$\frac{\partial \rho}{\partial t} + \frac{\partial}{\partial x_\ell}[\rho u_\ell] = 0 \tag{3a}$$

$$\rho T \frac{Ds}{Dt} = \tau_{m\ell} S_{m\ell} - \frac{\partial q_\ell}{\partial x_\ell} \tag{3b}$$

can be combined using these thermodynamic relations (1) to give

$$\frac{Dp}{Dt} = -\rho a^2 \frac{\partial u_\ell}{\partial x_\ell} + \lambda_{\rm G}\left(\tau_{m\ell} S_{m\ell} - \frac{\partial q_\ell}{\partial x_\ell}\right) \tag{3c}$$

$$\rho c_p \frac{DT}{Dt} = -\rho \beta_p T a^2 \frac{\partial u_\ell}{\partial x_\ell} + (1 + \lambda_{\rm G} \beta_p T)\left(\tau_{m\ell} S_{m\ell} - \frac{\partial q_\ell}{\partial x_\ell}\right) \tag{3d}$$

$$\rho \frac{Dh}{Dt} = -\rho a^2 \frac{\partial u_\ell}{\partial x_\ell} + (1 + \lambda_{\rm G})\left(\tau_{m\ell} S_{m\ell} - \frac{\partial q_\ell}{\partial x_\ell}\right) \tag{3e}$$

The above equations (3) are valid for general thermodynamic relations $p = p(\rho, T)$ and $c_p = c_p(\rho, T)$. Notice that the volume forces $f_{{\rm V}_i}$ present in the momentum equation, do not appear explicitly in the transport equations for the static thermodynamic variables ρ (3a), s (3b), p (3c), T (3d), or h (3e).

What appears clearly in (3) is that the transport of p, T or h is equal to the sum of a velocity-divergence-term (compressible, always scaling with a^2) and an entropy-production-term.

These equations can be easily manipulated to obtain transport equations for the variances of the static thermodynamic quantities (Gerolymos et al., 2007a,b,

2008). These were studied in previous work (Gerolymos et al., 2007a,b, 2008) for a limited range of Re_{τ_w} and $\bar{M}_{\rm CL}$. In the present work we extend this database and include time-series analysis.

2 DNS Database

The DNS data (Fig. 1) were generated by a finite-volume DNS solver (Gerolymos et al., 2009b) using an $O(\Delta x^{17})$ upwind-biased scheme (Gerolymos et al., 2009c). The method has been extensively validated by comparison of statistics and spectra with available compressible and incompressible pseudo-spectral DNS data (Gerolymos et al., 2009b). The solver is part of an open source project (Gerolymos and Vallet, 2009) and can be downloaded at http://sourceforge.net/projects/aerodynamics/.

3 Statistics and Scalings

Statistics (1-point and 2-point) were obtained for various $Re_{\tau_w} \in [100, 600]$ and $\bar{M}_{\rm CL} \in [0.3, 2.5]$ (although the simulations for $Re_{\tau_w} \approx 500$ are not well resolved). All of the basic 1-point statistics are well-converged (Fig. 1). The sampling frequency for the 1-point statistics was Δt^{-1} (sampling at every time-step) and for the 2-point statistics, from which spectra were computed, was $\frac{1}{100}\Delta t^{-1}$ (sampling every 100 time-steps).

Re_{τ_w}	$\bar{M}_{\rm CL}$	$N_x \times N_y \times N_z$	L_x	L_y	L_z	Δx^+	Δy_w^+	$N_{y^+\le 10}$	$\Delta y_{\rm CL}^+$	Δz^+	Δt^+	$t_{\rm ons}^+$
227	1.50	$345\times137\times529$	$8\pi\delta$	2δ	$4\pi\delta$	16.6	0.23	19	5.6	5.4	16.6×10^{-3}	1001
100	1.64	$137\times113\times201$	$8\pi\delta$	2δ	$4\pi\delta$	18.5	0.17	22	3.1	6.2	11.7×10^{-3}	3235
550	1.49	$177\times137\times265$	$8\pi\delta$	2δ	$4\pi\delta$	78.0	0.24	17	14.4	26.0	22.7×10^{-3}	2734
475	2.42	$177\times137\times265$	$8\pi\delta$	2δ	$4\pi\delta$	76.3	0.24	17	14.0	25.4	10.8×10^{-3}	1251
169	1.51	$257\times129\times385$	$8\pi\delta$	2δ	$4\pi\delta$	16.6	0.21	21	4.7	5.5	15.0×10^{-3}	1373
180	0.34	$257\times129\times385$	$8\pi\delta$	2δ	$4\pi\delta$	17.6	0.23	20	5.0	5.8	6.5×10^{-3}	592

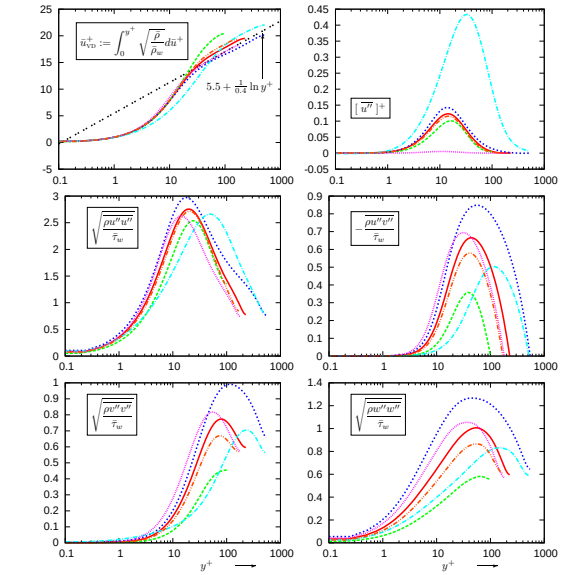

Figure 1: Comparison of computed turbulence statistics (van Driest-transformed velocity $\bar{u}^+_{\rm VD}$, $\overline{u''}$, $\overline{\rho u''_i u''_j}$) from present DNS computations using the UW17–C02 schemes, for various $Re_{\tau_w} \in [100, 600]$ and $\bar{M}_{\rm CL} \in [0.3, 2.5]$ (isothermal walls).

The relative fluctuation level of the thermodynamic quantities, $\rho'_{\rm rms}\bar\rho^{-1}$, $T'_{\rm rms}\bar T^{-1}$ and $p'_{\rm rms}\bar p^{-1}$, scale reasonably well (Fig. 2), at fixed Re_{τ_w}, with the square of the centerline Mach-number $\bar M^2_{\rm CL}$. There is of course a Re_{τ_w} influence, at fixed $\bar M_{\rm CL}$, the fluctuation level increasing with Re_{τ_w} (Fig. 2). The scaling seems less satisfactory for the $Re_{\tau_w} \in [450, 550]$ simulations, but this is attributed to the fact that these simulations are not fully converged (a part of the observation time $t_{\rm OBS}$ across which the statistics were taken, included transient evolution of the simulation; statistics must be restarted) and that they were run on rather coarse grids (Fig. 2). Close examination of the peaks of the relative fluctuation levels of ρ' and T', located at $y^+ \in [8, 15]$ (Fig. 2), indicates that their precise location moves further away from the wall (in wall units) as $M_{\rm CL}$ increases, but is quite insensitive to Re_{τ_w}.

It is well known, since the early work of Coleman et al.(Coleman et al., 1995; Huang et al., 1995), that the combined influence of Re_{τ_w} and $\bar M_{\rm CL}$ on the Reynolds-stresses is more intracate (Fig. 1), especially for $\overline{\rho u''v''}$, because of the variation of μ with T.

Re_{τ_w}	$\bar{M}_{\rm CL}$	$N_x \times N_y \times N_z$	L_x	L_y	L_z	Δx^+	Δy_w^+	$N_{y^+\le 10}$	$\Delta y_{\rm CL}^+$	Δz^+	Δt^+	$t_{\rm ons}^+$
227	1.50	$345\times137\times529$	$8\pi\delta$	2δ	$4\pi\delta$	16.6	0.23	19	5.6	5.4	16.6×10^{-3}	1001
100	1.64	$137\times113\times201$	$8\pi\delta$	2δ	$4\pi\delta$	18.5	0.17	22	3.1	6.2	11.7×10^{-3}	3235
550	1.49	$177\times137\times265$	$8\pi\delta$	2δ	$4\pi\delta$	78.0	0.24	17	14.4	26.0	22.7×10^{-3}	2734
475	2.42	$177\times137\times265$	$8\pi\delta$	2δ	$4\pi\delta$	76.3	0.24	17	14.0	25.4	10.8×10^{-3}	1251
169	1.51	$257\times129\times385$	$8\pi\delta$	2δ	$4\pi\delta$	16.6	0.21	21	4.7	5.5	15.0×10^{-3}	1373
180	0.34	$257\times129\times385$	$8\pi\delta$	2δ	$4\pi\delta$	17.6	0.23	20	5.0	5.8	6.5×10^{-3}	592

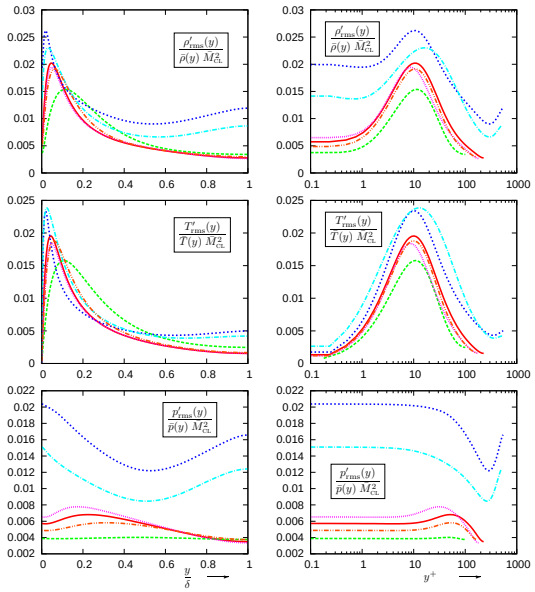

Figure 2: Scaling of temperature fluctuations for various $Re_{\tau_w} \in [100, 600]$ and $\bar{M}_{\rm CL} \in [0.3, 2.5]$ (isothermal walls).

4 Resolution and Box-size

Consideration of 1-D spectra in the homogeneous $x-$ (Fig. 3) and $z-$ (Fig. 4) directions highlights the resolution of the computations, while the analysis corresponding 2-point correlations, in homogeneous $x-$ (Fig. 5) and $z-$ (Fig. 6) directions, determines convergence of the statistics and box-size effects.

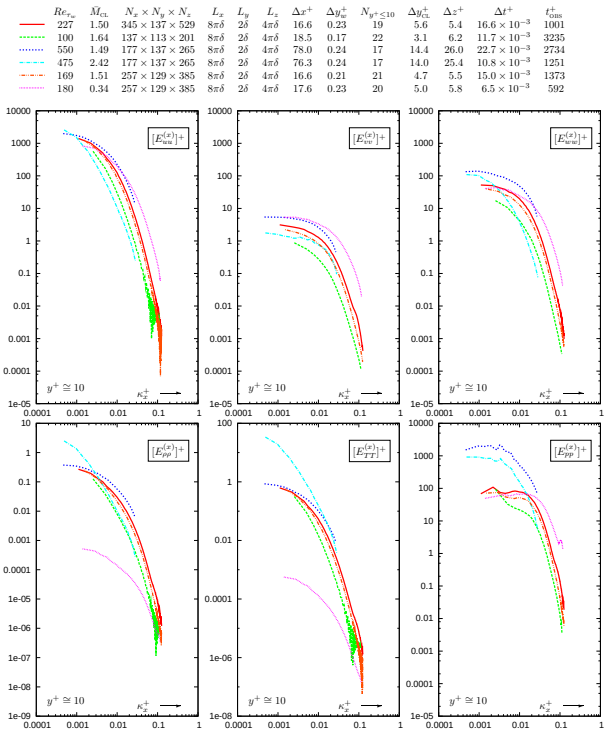

Figure 3: Computed 1-D spectra ($[E_{uu}^{(x)}]^+$, $[E_{vv}^{(x)}]^+$, $[E_{ww}^{(x)}]^+$, $[E_{\rho\rho}^{(x)}]^+$, $[E_{TT}^{(x)}]^+$, and $[E_{pp}^{(x)}]^+$) at $y^+ = 10.6$, for various $Re_{\tau_w} \in [100, 600]$ and $\bar{M}_{\text{CL}} \in [0.3, 2.5]$ (isothermal walls).

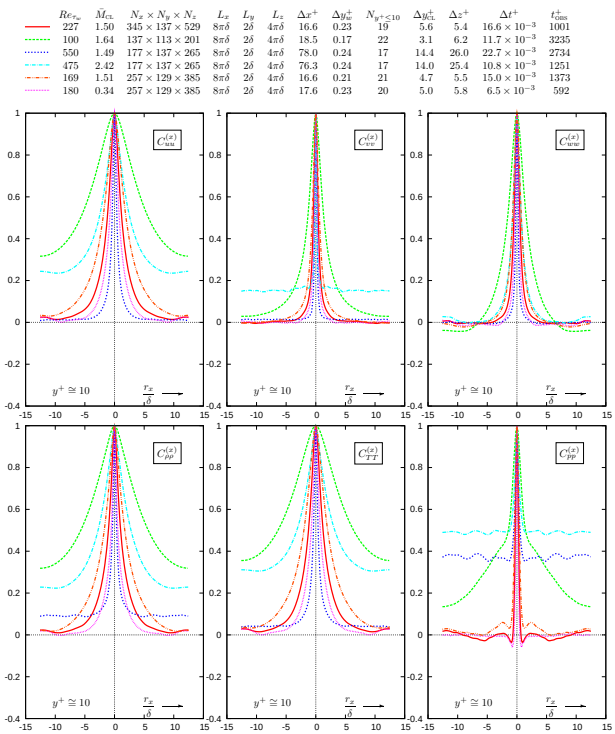

Figure 5: Computed 1-D 2-point correlation coefficients ($C_{uu}^{(x)}$, $C_{vv}^{(x)}$, $C_{ww}^{(x)}$, $C_{\rho\rho}^{(x)}$, $C_{TT}^{(x)}$, and $C_{pp}^{(x)}$) at $y^+ = 10.6$, for various $Re_{\tau_w} \in [100, 600]$ and $\bar{M}_{\text{CL}} \in [0.3, 2.5]$ (isothermal walls).

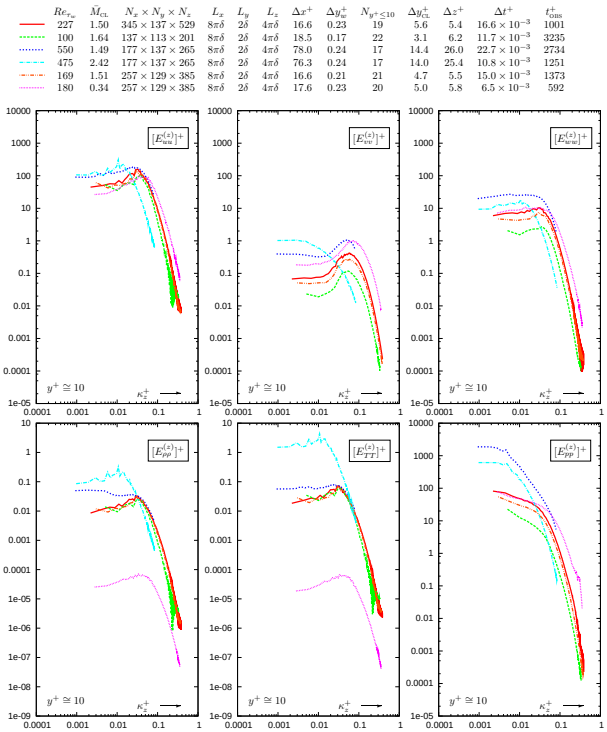

Figure 4: Computed 1-D spectra ($[E_{uu}^{(z)}]^+$, $[E_{vv}^{(z)}]^+$, $[E_{ww}^{(z)}]^+$, $[E_{\rho\rho}^{(z)}]^+$, $[E_{TT}^{(z)}]^+$, and $[E_{pp}^{(z)}]^+$) at $y^+ = 10.6$, for various $Re_{\tau_w} \in [100, 600]$ and $\bar{M}_{\text{CL}} \in [0.3, 2.5]$ (isothermal walls).

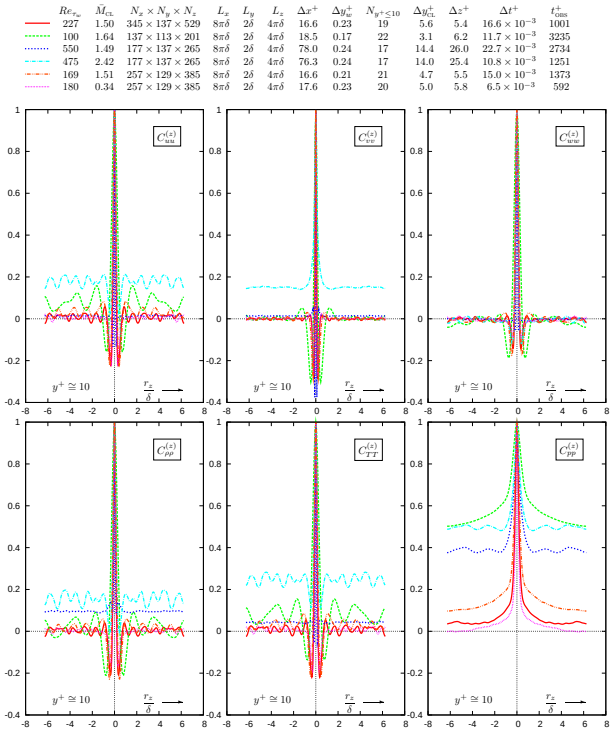

Figure 6: Computed 1-D 2-point correlation coefficients ($C_{uu}^{(z)}$, $C_{vv}^{(z)}$, $C_{ww}^{(z)}$, $C_{\rho\rho}^{(z)}$, $C_{TT}^{(z)}$, and $C_{pp}^{(z)}$) at $y^+ = 10.6$, for various $Re_{\tau_w} \in [100, 600]$ and $\bar{M}_{\text{CL}} \in [0.3, 2.5]$ (isothermal walls).

Obviously, the preliminary coarse grid $Re_{\tau_w} \approx 500$ computations are not well resolved (Figs. 3, 4), although the $\bar{M}_{\rm CL} = 2.42$ simulation is better resolved than the $\bar{M}_{\rm CL} = 1.50$ one, since the $\bar{M}_{\rm CL}$ increase shifts the spectra towards lower wavenumbers (Figs. 3, 4). A more important observation is that the logarithmic slope (exponent) of $E_{\rho\rho}$ (and E_{TT}) is strongly dependent on $\bar{M}_{\rm CL}$, in contrast to the velocity (E_{uu}, E_{vv}, E_{ww}) and pressure (E_{pp}) spectra whose slope in the inertial range seems relatively independent of $\bar{M}_{\rm CL}$. As a result, the energy level separation for $E_{\rho\rho}$ between the large and the smallest resolved scales, on a given grid, decreases with decreasing $\bar{M}_{\rm CL}$ much faster that the energy level separation for $E_{u_i u_i}$. Notice that, for $\bar{M}_{\rm CL} \approx 0.35$, the energy level separation between the large scales and the smallest grid resolved scales, is similar for E_{pp}, E_{TT} and $E_{\rho\rho}$. As a result, although as demonstrated by extensive comparisons with incompressible DNS data (Gerolymos et al., 2009b), the grid used for the ($Re_{\tau_w}, \bar{M}_{\rm CL}$)≅(180,0.35) computations is quite satisfactory for the prediction of velocity spectra, it is insufficient for examining in detail the density fluctuations (in particular the destruction of $\overline{\rho'^2}$ which occurs at the small scales). On the contrary the ($Re_{\tau_w}, \bar{M}_{\rm CL}$)≅(227,1.5) simulations are well resolved both for velocities and for thermodynamic quantities.

Consideration of 2-point correlation coefficients (Figs. 5, 6) highlights the well known effect of increase of correlation lengths (outer scaling) with decreasing Re_{τ_w}, suggesting the need of larger box size for the $Re_{\tau_w} \approx 100$ simulations. The unsatisfactory (high-level) correlation coefficient C_{pp} for the $Re_{\tau_w} \approx 500$ simulations (Figs. 5, 6) is attributed to the presence of transients in these simulations (statistics were restarted to exclude this transient).

5 Density variance and massflux

The transport equations for the density variance $\overline{\rho'^2}$ (4) and for the massflux $\bar{\rho}\widetilde{u_i''} = -\overline{\rho' u_i''}$ (5) were given by Taulbee and VanOsdol (1991).

$$\underbrace{\frac{\partial \overline{\rho'^2}}{\partial t} + \tilde{u}_\ell \frac{\partial \overline{\rho'^2}}{\partial x_\ell}}_{\text{convection } C_{(\rho')}} = \underbrace{\frac{\partial \left(-\overline{\rho'^2 u_\ell''} \right)}{\partial x_\ell}}_{\text{diffusion } d_{(\rho')}}$$
$$\underbrace{-2\overline{\rho' u_\ell'} \frac{\partial \bar{\rho}}{\partial x_\ell} - 2\overline{\rho'^2} \frac{\partial \tilde{u}_\ell}{\partial x_\ell}}_{\text{production } P_{(\rho')} := P_{(\rho';\nabla\bar{\rho})} + P_{(\rho';\breve{\Theta})}}$$
$$\underbrace{- \left[\overline{(\rho^2 - \bar{\rho}^2) \frac{\partial u_\ell''}{\partial x_\ell}} \right]}_{\text{destruction } \varepsilon_{(\rho')}} = 0 \qquad (4)$$

$$\underbrace{\frac{\partial}{\partial x_\ell}(\overline{\rho' u_i'' u_\ell''})}_{\rm I} \underbrace{-\bar{\rho}\frac{\partial \tilde{u}_i}{\partial x_\ell}}_{\rm II} \underbrace{+\overline{u_i'' u_\ell''}\frac{\partial \bar{\rho}}{\partial x_\ell}}_{\rm III} \underbrace{+\bar{\rho}\overline{u_i''\frac{\partial u_\ell''}{\partial x_\ell}}}_{\rm IV}$$
$$\underbrace{-\overline{\left(\frac{\bar{\rho}}{\rho} - 1\right)\frac{\partial p}{\partial x_i}}}_{\rm V} \underbrace{+\overline{\left(\frac{\bar{\rho}}{\rho} - 1\right)\frac{\partial \tau_{i\ell}}{\partial x_\ell}}}_{\rm VI} \underbrace{+\bar{\rho}\overline{f_{{\rm V}_i}''}}_{\rm VII} = 0 \qquad (5)$$

Surprisingly little work has been reported on extracting information from DNS computations on these basic transport equations of compressible turbulence. We have recently studied the budgets (Gerolymos et al., 2007a) and sketched some initial attempts for the *a priori* modeling (Gerolymos et al., 2008) of the $\overline{\rho'^2}$ transport equation (4).

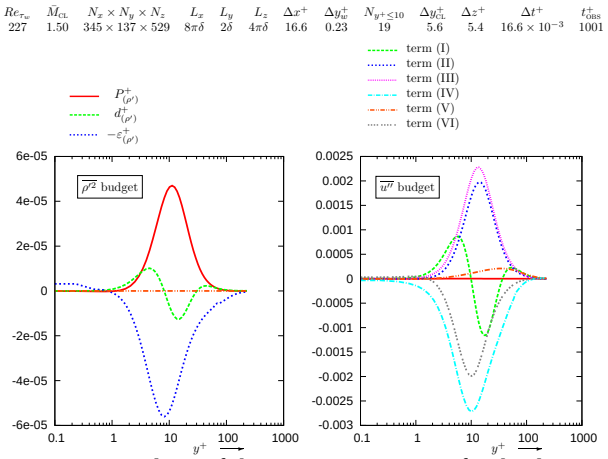

Figure 7: Budgets of the transport equations for the density variance $\overline{\rho'^2}$ (4), and for the streamwise massflux $\overline{u''}$ (5), in wall units, from present DNS computations using the UW17–C02 scheme ($Re_{\tau_w} = 227$, $\bar{M}_{\rm CL} = 1.5$, isothermal walls), on $347 \times 137 \times 529$ grid.

We consider also in the present work, budgets (Fig. 7) of the streamwise massflux $\overline{u_i''}$ transport equation (5). It appears from these budgets that the fluctuating velocity-dilataion correlation term IV in (5) is a destruction term in the plane channel flow considered in the present work, even more important than the term VI in (5) which contains together viscous diffusion and destruction through viscosity effects. The fluctuating specific-volume/pressure-gradient correlation term V in (5) does not seem important for the flow considered.

6 Time-Series and 2-time Correlations

We have extracted time-series of the 5 primitive variables at 6 $y^+ = \text{cost}$ locations (including the walls $y^+ = 0$ and the symmetry-plane $y^+ = Re + \tau_w$), for every other point in the x and z directions (Fig. 8). Sampling frequency was $f_s = \Delta t^{-1}$. Results are being processed to obtain frequency spectra and 2-time

correlations. As an example we present very preliminary results with the UW17 scheme on the $129 \times 129 \times 129$ grid using the e_0DTSBDF2, e_0DTSBDF3 and e_0DTSBDF4, and the RK4 time-integration methods (Gerolymos et al., 2009a). The observation times that were processed are rather short, but sufficient to show the similarity of the results between the methods, but also the basic trends in the results. We consider (Fig. 9) 2-time correlations ${}^{(t)}R_{u_iu_j}(\vec{x},t,r_t) := \overline{u'_i(\vec{x},t)u'_j(\vec{x},t+r_t)}$, and corresponding frequency-spectra. The 2-time-correlations were obtained by averaging of 48 spatial points (the database on each plane for this grid contains 2048 spatial points, but only 48 were used for these preliminary results. The observation time seems adequate for ${}^{(t)}R_{vv}$ and ${}^{(t)}R_{ww}$, but not for ${}^{(t)}R_{uu}$ (Fig. 9). This explains why there is more noise in the frequency-spectra ${}^{(t)}E_{uu}$, while ${}^{(t)}R_{vv}$ and ${}^{(t)}R_{ww}$ are much smoother. What is important is that the results with all of the 4 methods are very similar, including these temporal data. The frequency-spectra obtained are in very good agreement with the experimental spectra of Fernholz et al. (Fernholz et al., 1995) (obtained at much higher y^+ and Re_θ). It seems that time-integration is not as crucial to the quality of the results as the spatial discretization of the convective terms.

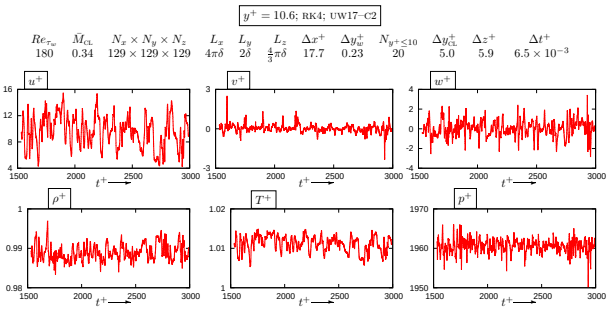

Figure 8: Typical time-series of u^+, v^+, w^+, ρ^+, T^+, and p^+, at a point located at $y^+ = 10.6$, from present DNS computations using the UW17–C02 scheme and the RK4 time-integration method ($Re_{\tau_w} = 180$, $\bar{M}_{CL} = 0.35$, isothermal walls), on $129 \times 129 \times 129$ grid.

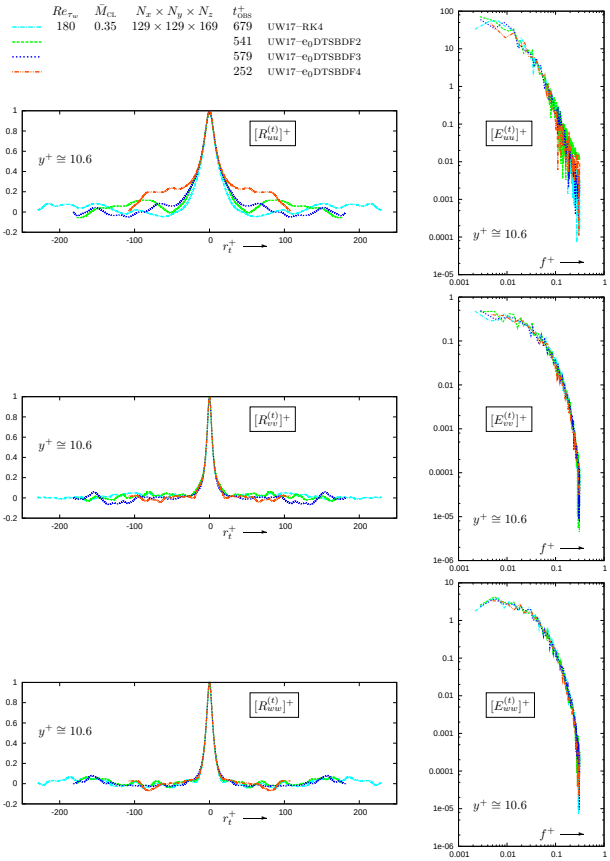

Figure 9: Comparison of computed 2-time correlations and time-spectra ($[E^{(t)}_{uu}]^+$, $[E^{(t)}_{vv}]^+$, $[E^{(t)}_{ww}]^+$) at $y^+ = 10.6$, from present DNS computations using the UW17–C02 scheme and the e_0DTSBDF2, e_0DTSBDF3 and e_0DTSBDF4, and the RK4 time-integration methods ($Re_{\tau_w} = 180$, $\bar{M}_{CL} = 0.35$, isothermal walls), on $129 \times 129 \times 129$ grid.

7 Conclusions and Perspectives

Grid resolution requirements in DNS simulations of compressible wall-turbulence are more strigent than those necessary for studying velocity fluctuations, especially as $\bar{M}_{CL}$ decreases approaching the very weakly compressible turbulence limit. For $\bar{M}_{CL} \approxeq 1.5$ and $Re_{\tau_w} \in [180, 230]$ we have constructed a well resolved database for the transport equations of quantities related to the fluctuations of thermodynamic quantities, and presented examples for the budgets of density-variance and massflux.

We have also presented preliminary results for other values of $\bar{M}_{CL}$ and Re_{τ_w}, which are part of an ongoing effort towards constructing a compressible channel flow DNS database, with emphasis on the behaviour of thermodynamic quantities (http://www.aerodynamics.fr) using an open source DNS solver (Gerolymos and Vallet, 2009).

Acknowledgments

The present work was partly supported by the EU-funded research project ProBand, (STREP–FP6 AST4–CT–2005–012222). Computations were performed using HPC resources from GENCI–IDRIS (Grants 2007–066327, 2008–066327, 2009–066327, 2010–066327, and 2010–022139).

References

ARP V., PERSICHETTI J.M., GUO-BANG C. (1984) : The Grüneisen Parameter in Fluids, *ASME J. Fluids Eng.* **106** 193–201.

COLEMAN G.N., KIM J., MOSER R.D. (1995) : A Numerical Study of Turbulent Supersonic Isothermal-Wall Channel Flow,

J. Fluid Mech. **305** 159–183.

FERNHOLZ H.H., KRAUSE E., NOCKEMANN M., SCHOBER M. (1995) : Comparative Measurements in the Canonical Boundary-Layer at $Re_{\delta_2} \leq 6 \times 10^4$ on the Wall of the German-Dutch Windtunnel, *Phys. Fluids* **7** 1275–1281.

FRIEDRICH R. (2007) : Compressible Turbulent Flows: Aspects of Prediction and Analysis, *Z. ang. Math. Mech.* **87** 189–211.

GEROLYMOS G.A., SÉNÉCHAL D., VALLET I. (2007a) : Pressure, Density and Temperature Fluctuations in Compressible Turbulent Flow — I, AIAA Paper 2007–3408, 13. AIAA/CEAS Aeroacoustics Conference, 21–23 may 2007, Roma [ITA].

GEROLYMOS G.A., SÉNÉCHAL D., VALLET I. (2007b) : Wall-Effects on Pressure Fluctuations in Quasi-Incompressible and Compressible Turbulent Plane Channel Flow, AIAA Paper 2007–3863, 37. AIAA Fluid Dynamics Conference, 25–28 jun 2007, Miami [FL, USA].

GEROLYMOS G.A., SÉNÉCHAL D., VALLET I. (2008) : Pressure, Density and Temperature Fluctuations in Compressible Turbulent Flow – II – *A priori* Modelling of the Density Variance, AIAA Paper 2008–0647, 46. Aerospace Sciences Meeting, 7–10 jan 2008, Reno [NV, USA].

GEROLYMOS G.A., SÉNÉCHAL D., VALLET I. (2009a) : Analysis of Dual-Time-Stepping with Explicit Subiterations, AIAA Paper 2009–1608, 47. Aerospace Sciences Meeting, 5–8 jan 2009, Orlando [FL, USA].

GEROLYMOS G.A., SÉNÉCHAL D., VALLET I. (2009b) : Performance of Very-High-Order Upwind Schemes for DNS of Compressible Wall-Turbulence, *Int. J. Num. Meth. Fluids* [in print; published online jul 2009: DOI: 10.1002/fld.2096].

GEROLYMOS G.A., SÉNÉCHAL D., VALLET I. (2009c) : Very-High-Order WENO Schemes, *J. Comp. Phys.* **228** 8481–8524.

GEROLYMOS G.A., VALLET I. (2009) : aerodynamics (a package for computational aerodynamics), http://sourceforge.net/projects/aerodynamics.

HUANG P.G., COLEMAN G.N., BRADSHAW P. (1995) : Compressible Turbulent Channel Flows: DNS Results and Modelling, *J. Fluid Mech.* **305** 185–218.

RUBINSTEIN R., ERLEBACHER G. (1997) : 2-Component Limit, *Phys. Fluids* **9** 3037–3057.

TAULBEE D., VANOSDOL J. (1991) : Modeling Turbulent Compressible Flows: The Mass Fluctuating Velocity and Squared Density, AIAA Paper 1991–0524.

WU M., MARTÍN M.P. (2007) : Direct Numerical Simulation of Supersonic Turbulent-Boundary-Layer over a Compression-Ramp, *AIAA J.* **45** 879–889.